Electrostatic contribution to twist rigidity of DNA

Farshid Mohammad-Rafiee* and Ramin Golestanian†
Institute for Advanced Studies in Basic Sciences, Zanjan 45195-159, Iran
(Received 15 December 2003; published 22 June 2004)

The electrostatic contribution to the twist rigidity of DNA is studied, and it is shown that the Coulomb self-energy of the double-helical sugar-phosphate backbone makes a considerable contribution—the electrostatic twist rigidity of DNA is found to be $C_{\mathrm{elec}} \approx 5$ nm, which makes up about 7% of its total twist rigidity ($C_{\mathrm{DNA}} \approx 75$ nm). The electrostatic twist rigidity is found, however, to depend only weakly on the salt concentration, because of a competition between two different screening mechanisms: (1) Debye screening by the salt ions in the bulk, and (2) structural screening by the periodic charge distribution along the backbone of the helical polyelectrolyte. It is found that, depending on the parameters, the electrostatic contribution to the twist rigidity could stabilize or destabilize the structure of a helical polyelectrolyte.

DOI: 10.1103/PhysRevE.69.061919 PACS number(s): 87.15.−v, 36.20.−r, 61.41.+e

I. INTRODUCTION

Genetic information in living cells is carried in the double-helical linear sequence of nucleotides in DNA. The DNA double helix can be found in several forms that differ from each other in geometrical characteristics such as diameter and handedness. Under normal physiological conditions, DNA adopts the *B* form, in which it consists of two helically twisted sugar-phosphate backbones with diameter 2.4 nm, which are stuffed with base pairs and are located asymmetrically with respect to each other as characterized by the presence of major and minor grooves. The helix is right handed with ten base pairs per turn, and the pitch of the helix is 3.4 nm [1].

It is well known that above *p*H 1 each phosphate group in DNA has a negative charge [2], which renders the polymer stiff due to the electrostatic repulsion between these groups. The presence of neutralizing counterions and salt in the solvent screens the electrostatic repulsion, thereby leading to an effective way of controlling the stiffness of polyelectrolytes via the ionic strength of the solution. To account for the electrostatic stiffening, Odijk [3], and Skolnick and Fixman [4] adopted an effective wormlike chain description for the bending elasticity of stiff polyelectrolytes and calculated the correction to the persistence length due to the electrostatic interactions. The so-called electrostatic persistence length is found to be proportional to the square of the Debye screening length, implying that the stiffness of polyelectrolytes such as DNA should be very sensitive to the salt concentration [5]. While there are experiments that measure the electrostatic contribution to the bending rigidity of DNA in various salt concentrations [6,7], it is generally believed that changing the ionic strength has no significant effect on the rigidity of DNA under most physiologically relevant conditions [8]. Hence, in this so-called salt saturation limit, the bending rigidity of DNA is entirely due to the mechanical stiffness of the double-helical backbone.

Similar studies have shown that the twist rigidity of DNA is also relatively insensitive to the ionic strength of the solution [9]. This experimental finding is usually explained by saying that (unlike bending) twisting a polyelectrolyte does not change the distance between the different charges on its backbone appreciably, and thus it is not affected by electrostatic interactions [10]. Here, we set out to reconsider this line of argument and attempt to account for the above experimental observation from a different point of view. We consider the electrostatic self-interaction of the double-helical sugar-phosphate backbone (see Fig. 1) and show that the periodic arrangement of the charge distribution effectively screens the electrostatic interaction, with the screening length given by the pitch of the DNA. In other words, cor-

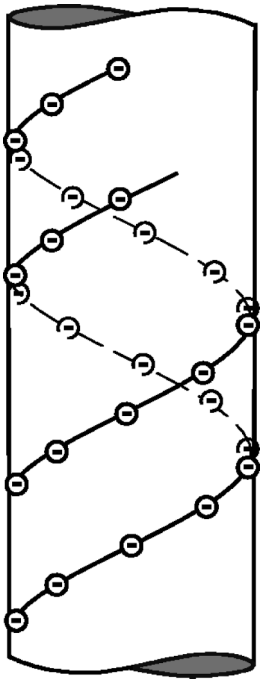

FIG. 1. A schematic picture of double-helical *B*-DNA with the negative charges lying on the sugar-phosphate backbone in a periodic manner.

*Electronic address: farshidm@iasbs.ac.ir
†Electronic address: golestan@iasbs.ac.ir

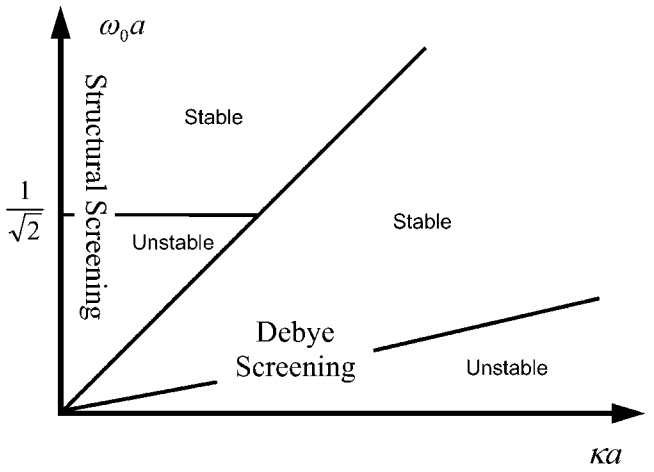

FIG. 2. The diagram delineating the different regimes in the parameter space of a helical polyelectrolyte, where $\omega_0=2\pi/P$, and a is the radius of the helix. The line separating the two screening regimes has slope 1, whereas the slope of the boundary denoting the onset of instability in the Debye screening regime is set by the inverse of a cutoff number n_c (see below). A stable (unstable) state corresponds to positive (negative) electrostatic twist rigidity only. The overall stability of the macromolecule, however, is determined by the total twist rigidity which consists of both mechanical and electrostatic contributions (see Sec. IV).

responding to such a periodic charge distribution, there are two competing screening lengths: (1) the Debye screening length of the bulk solution κ^{-1} that is controlled by the ionic strength, and (2) the period of the charge distribution P, and it is the smaller of these two lengths that controls the range of Coulomb interaction. We find that electrostatic interactions make an appreciable contribution to the twist rigidity of DNA, although it depends only weakly on the Debye screening length as long as this length is larger than the DNA pitch. We study the effect of various geometrical parameters such as the diameter of the double helix, the distance between the two helices, and the pitch, as well as the Debye screening length, on the electrostatic contribution to the twist rigidity and show that it can be either positive or negative depending on the values of these parameters. The results are summarized in Fig. 2, where a diagram is sketched in the parameter space delineating all the different regimes.

The rest of the paper is organized as follows. Section II describes the model that is used to study the electrostatic contribution to the twist rigidity of DNA, followed by a presentation of the results in Sec. III. Finally, Sec. IV concludes the paper, while some details of the calculations appear in three Appendixes.

II. THE MODEL

To study the effect of electrostatic interactions on the twist rigidity of DNA, we consider a simple model in which the sugar-phosphate charged backbone of each DNA strand is assumed to wrap around a cylinder of radius a in a helical manner, as shown in Fig. 1. The double helix can then be viewed as a cylinder with a surface charge density $\sigma(z,\theta)$ corresponding to the negative charges, whose electrostatic self-energy can be calculated as

$$E_{\rm elec}=\frac{a^2}{2}\int dzdz'\int_0^{2\pi} d\theta d\theta'\,\sigma(z,\theta)\sigma(z',\theta') \times V_{\rm DH}(|\vec{r}(z,\theta)-\vec{r}(z',\theta')|), \tag{1}$$

where $\vec{r}(z,\theta)$ parametrizes the position on the surface of the cylinder with z being the coordinate along the axis and θ being the polar angle. The effective pair potential between two charges in the solution is given by the Debye-Hückel interaction [11]

$$V_{\rm DH}(r)=k_{\rm B}T\frac{\ell_{\rm B}}{r}e^{-\kappa r}, \tag{2}$$

where $\ell_{\rm B}=e^2/(\epsilon k_{\rm B}T)$ is the Bjerrum length, and κ^{-1} is the Debye screening length, defined via [1]

$$\kappa^2=4\pi\ell_{\rm B}\sum_i Z_i^2 c_i, \tag{3}$$

where Z_i and c_i are the valence and the concentration of the salt species i, respectively, and the summation is over the ionic species in the solution. The effect of counterion condensation, which is neglected in this simple Debye-Hückel theory, will be discussed later in Sec. IV.

Due to the helical structure of DNA, $\sigma(z,\theta)$ is a doubly periodic function, namely, $\sigma(z,\theta)=\sigma(z+P,\theta)=\sigma(z,\theta+2\pi)$, where P is the helix pitch. Therefore, it is convenient to write $\sigma(z,\theta)$ in the Fourier space as

$$\sigma(z,\theta)=\sum_{m,n}\sigma_{mn}e^{i(2\pi m/P)z+in\theta}, \tag{4}$$

where m and n are integer numbers.

Making use of the periodicity of the charge distribution, one can simplify the form of the electrostatic self-energy of Eq. (1) using the Fourier representation of the screened Coulomb interaction. After some manipulation, whose details can be found in Appendix A, one finds

$$\beta E_{\rm elec}=4\pi^2\ell_{\rm B}La^2\sum_{m,n}|\sigma_{m,n}|^2 I_n[\sqrt{(\kappa a)^2+(na\omega_0)^2}] \times K_n[\sqrt{(\kappa a)^2+(na\omega_0)^2}], \tag{5}$$

where $\beta=1/(k_{\rm B}T)$, $\omega_0=2\pi/P$ is the spontaneous twist of the helix, and L is the overall length of the macromolecule.

We now focus on the specific case of DNA, whose charge density $\sigma(z,\theta)$ can be written as (see Fig. 3)

$$\sigma(z,\theta)=-\frac{P}{2\pi ab}\left[\delta\left(z-\frac{P\theta}{2\pi}\right)+\delta\left(z-\zeta-\frac{P\theta}{2\pi}\right)\right], \tag{6}$$

where b is the vertical distance between two charges in a strand, and ζ is the distance between the two strands along the z direction, as shown in Fig. 3. Note that

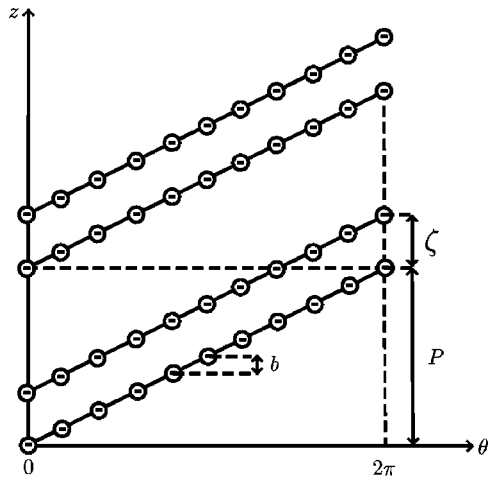

FIG. 3. A schematic picture of the surface charge distribution of *B*-DNA. The geometrical parameters of DNA are shown in the picture: b is the vertical distance between two successive charges on each strand, ζ is the distance between the two strands along the z axis (given by the width of the minor groove in *B*-DNA), and P is the pitch of the helix.

$$\int_0^P dz \int_0^{2\pi} ad\theta\sigma(z,\theta) = -\frac{2P}{b} \tag{7}$$

yields the number of charges in each repeat unit of DNA. The Fourier transform of the charge density $\sigma_{m,n}$ can now be calculated from Eqs. (4) and (6) as

$$\sigma_{m,n} = -\frac{1}{2\pi ab}\delta_{m,-n}[1 + e^{in\omega_0\zeta}], \tag{8}$$

using which the electrostatic self-energy of the double-helical DNA can be calculated [from Eq. (5)] as

$$\beta E_{\text{elec}}(\omega_0) = \frac{4\ell_B L}{b^2}\sum_{n=0}^{\infty\prime}(1+\cos\, n\omega_0\zeta)\times I_n[\sqrt{(\kappa a)^2+(na\omega_0)^2}] \times K_n[\sqrt{(\kappa a)^2+(na\omega_0)^2}], \tag{9}$$

where the prime indicates that the $n=0$ term should be counted with a prefactor of $1/2$.

To calculate the contribution to the twist rigidity from the above Coulomb interaction, we impose an additional uniform twist of Ω in the double helix and calculate the change in the self-energy, i.e., $\beta E_{\text{elec}}(\omega_0+\Omega)-\beta E_{\text{elec}}(\omega_0)$. Expanding the energy change in powers of Ω, we can then read off the electrostatic twist rigidity as

$$C_{\text{elec}} = \left.\frac{1}{L}\frac{\partial^2\beta E_{\text{elec}}}{\partial\Omega^2}\right|_{\Omega=0}, \tag{10}$$

subject to the constraint that the relative positioning of the two helical strands should not alter upon deformation. This is a plausible assumption, which implies that the parameter ζ changes accordingly to ζ' such that $(\omega_0+\Omega)\zeta'=\omega_0\zeta$.

The total energy, which is the sum of the mechanical and electrostatic contributions, can be written as

$$\beta E_{\text{tot}} = \beta E_{\text{elec}}(\omega_0+\Omega) + \frac{1}{2}\int_0^L ds\; C_{\text{mech}}\Omega^2, \tag{11}$$

where C_{mech} is the mechanical twist rigidity [12]. When an additional uniform twist of Ω is imposed on the double helix, the total energy can be written in a simple form as

$$\beta E_{\text{tot}} = \frac{1}{2}L\; C_{\text{mech}}\Omega^2 + \beta E_{\text{elec}}(\omega_0) + LW_{\text{elec}}\Omega + \frac{1}{2}L\; C_{\text{elec}}\Omega^2 + O(\Omega^3), \tag{12}$$

where W_{elec} is defined as

$$W_{\text{elec}} \equiv \left.\frac{1}{L}\frac{\partial\beta E_{\text{elec}}}{\partial\Omega}\right|_{\Omega=0}. \tag{13}$$

III. THE RESULTS

Under normal physiological conditions, $\kappa\approx 1\ \text{nm}^{-1}$ and the spontaneous twist of *B*-DNA is $\omega_0=1.85\ \text{nm}^{-1}$. Since the closed form calculation of C_{elec} and W_{elec} from Eqs. (9), (10), and (13) is cumbersome, we choose to expand the modified Bessel functions I_n and K_n to fourth order in $(\kappa a)/(na\omega_0)$. This approximation appears to yield sufficient accuracy for the experimentally relevant range of parameters.

A. Correction to twist rigidity

To calculate C_{elec}, it is convenient to use the asymptotic forms of $I_n(nx)$ and $K_n(nx)$ for sufficiently large n. We find that $I_n(nx)K_n(nx)=(1/2n)(1/\sqrt{1+x^2})+O(1/n^{2+\delta})$ with $\delta\geqslant 0$, and observe that to a good approximation one can just use the relevant asymptotic forms of I_n and K_n for $n\geqslant 2$, in calculating the electrostatic twist rigidity (see Appendix B for details). We find

$$C_{\text{elec}} = \frac{2\ell_B a^2}{b^2}(1+\cos\,\omega_0\zeta)\times[f_0(a\omega_0) - f_2(a\omega_0)(\kappa a)^2 + f_4(a\omega_0)(\kappa a)^4] + \frac{2\ell_B a^2}{b^2}\frac{(2a^2\omega_0^2-1)}{(a^2\omega_0^2+1)^{5/2}} \times\sum_{n=2}^{\infty}\frac{1}{n}(1+\cos\, n\omega_0\zeta), \tag{14}$$

where $f_0(x)$, $f_2(x)$, and $f_4(x)$ are functions defined in Appendix C. The first term in the above equation corresponds to the lowest mode of the self-energy, and comes from the electrostatic interactions between the charges that are positioned on different domains. The expansion in κa is meant to capture the Debye screening correction. The rest is the contribution from higher modes that constitute electrostatic interactions between charges that are closer to each other, and appears to smear out the Debye screening correction more strongly than the lowest mode contribution.

The coefficient of the summation term in Eq. (14) shows the possibility of a sign change when $a\omega_0=1/\sqrt{2}$. This can be understood as a competition between the instability due to

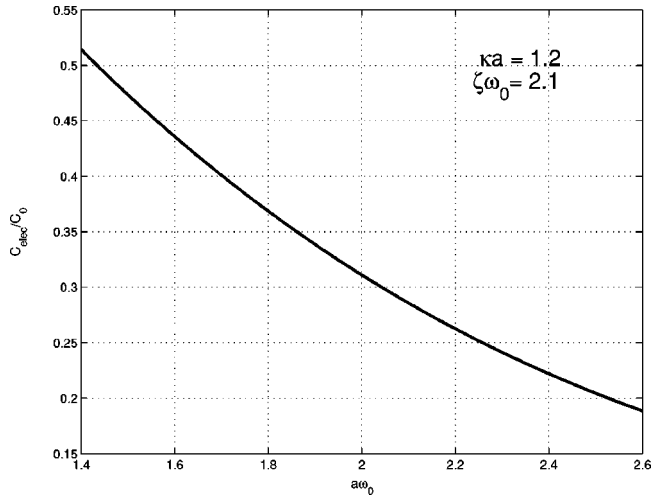

FIG. 4. C_{elec}/C_0 as a function of $a\omega_0$. This plot corresponds to $\kappa a=1.2$ and $\zeta\omega_0=2.1$.

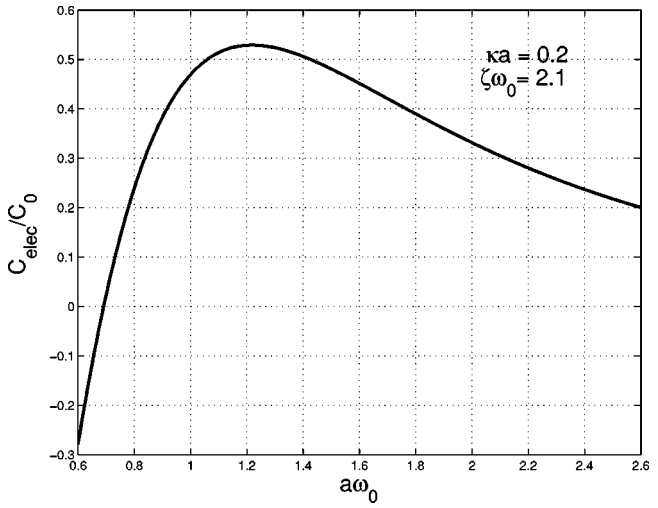

FIG. 5. C_{elec}/C_0 as a function of $a\omega_0$. This plot corresponds to $\kappa a=0.2$ and $\zeta\omega_0=2.1$.

the so-called Earnshaw theorem [13], which is inherent to a collection of electrostatic point charges in any space configuration, and the structural screening, which tends to remove this instability.

In the summation term in Eq. (14) above, where we have used the asymptotic forms of the Bessel functions, no dependence on κ remains and only the structural parameters of DNA such as a and ω_0 enter. The summation diverges as $1/n$, and needs to be regularized with a cutoff for n, which can be estimated as $n_c=2\pi a/t$, where t is set by the thickness of each strand. Then Eq. (14) can be written as

$$C_{\mathrm{elec}}=\frac{2\ell_B a^2}{b^2}(1+\cos\,\omega_0\zeta)\times[f_0(a\omega_0)-f_2(a\omega_0)(\kappa a)^2 + f_4(a\omega_0)(\kappa a)^4]+\frac{2\ell_B a^2}{b^2}\frac{(2a^2\omega_0^2-1)}{(a^2\omega_0^2+1)^{5/2}} \times\left[\gamma+\ln\frac{n_c}{2\,\sin(\omega_0\zeta/2)}-(1+\cos\,\omega_0\zeta)\right], \qquad (15)$$

where $\gamma=0.577\,216$ is the Euler constant. Note that the above result, as we have already mentioned, is valid only for $\kappa<\omega_0$.

Let us first evaluate the overall magnitude of the electrostatic twist rigidity, as given by Eq. (15). For *B*-DNA, we have $a=1.2$ nm, $\omega_0=1.85$ nm^{-1}, $b=3.4$ Å, and $\zeta=1.13$ nm [2], and the Bjerrum length is given as $\ell_B=7.1$Å. Using these parameters and defining $C_0\equiv 2\ell_B a^2/b^2$, we find $C_0=174$ Å, which is relatively large. To estimate n_c for *B*-DNA, we use $t\approx 5$ Å, which gives $n_c\approx 15$. Using these estimates and $\kappa\approx 1$ nm^{-1}, Eq. (15) yields $C_{\mathrm{elec}}=46$ Å at the physiological salt concentration. This should be compared to the overall twist rigidity of *B*-DNA, which is believed to be about 75 nm [14].

To study the effect of various parameters, namely, the spontaneous twist, the diameter, and the asymmetry of the double helix, as well as the salt concentration, we choose to work with the three dimensionless parameters $a\omega_0$, κa, and $\zeta\omega_0$. In Fig. 4, the behavior of C_{elec} is shown as a function of $a\omega_0$ for $\kappa a=1.2$ and $\zeta\omega_0=2.1$. The domain for $a\omega_0$ is chosen such that the condition $\kappa<\omega_0$ is satisfied and Eq. (15) is valid. The plot shows that, for sufficiently high salt concentration, the electrostatic torsional stiffness decreases as the spontaneous twist of the double helix increases.

For sufficiently low salt concentration, however, it appears that the behavior is not always monotonic, as shown in Fig. 5, where C_{elec} is plotted as a function of $a\omega_0$ for $\kappa a=0.2$ and $\zeta\omega_0=2.1$. Interestingly, one can see that C_{elec} can even become negative, due to the fact that in Eq. (15) the first term becomes relatively weak for low salt concentrations and the second term, which is dominant, changes sign for $a\omega_0<1/\sqrt{2}$.

In Fig. 6, the dependence of C_{elec} is shown on the asymmetry parameter $\zeta\omega_0$ for $\kappa a=1.2$ and $a\omega_0=2.2$. One observes that, for the relatively large window of $0.4\pi\leqslant\zeta\omega_0\leqslant 1.6\pi$, C_{elec} is almost constant, and is thus not sensitive to the relative positioning of the two strands. For $\zeta\omega_0=0$ and 2π, a divergence sets in due to the fact that the charges on the two strands develop contacts with each other.

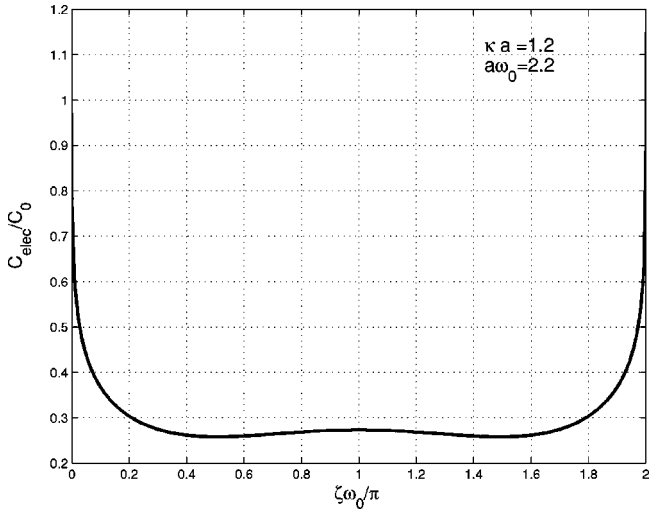

FIG. 6. C_{elec}/C_0 as a function of $\zeta\omega_0/\pi$. This plot corresponds to $\kappa a=1.2$ and $a\omega_0=2.2$.

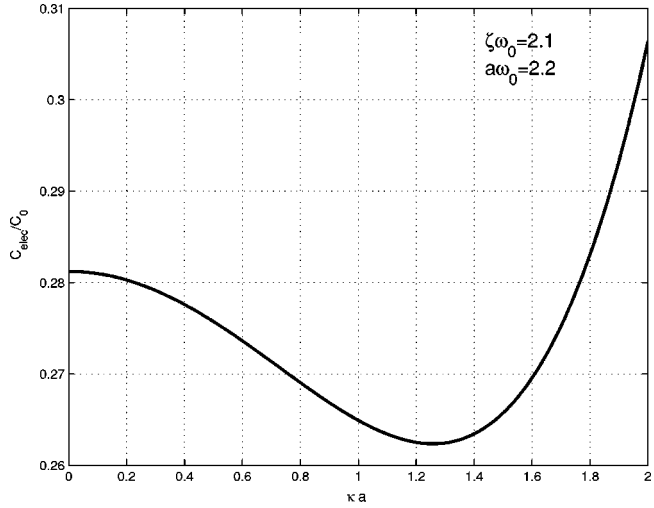

FIG. 7. $C_{\rm elec}/C_0$ as a function of κa. This plot corresponds to $\zeta\omega_0=2.1$ and $a\omega_0=2.2$.

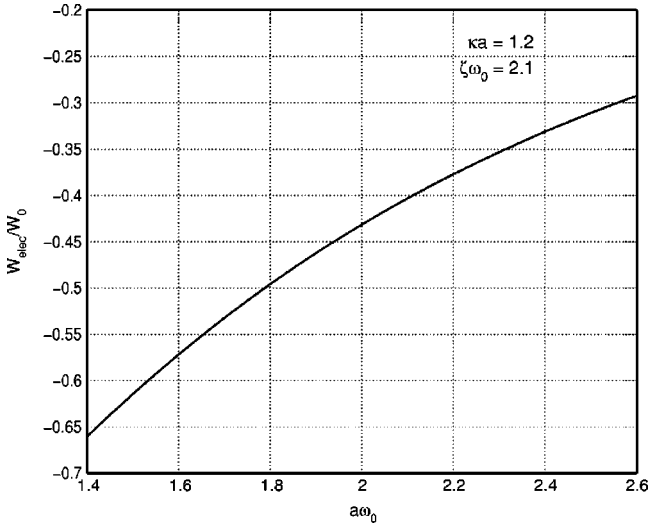

FIG. 8. $W_{\rm elec}/W_0$ as a function of $a\omega_0$. This plot corresponds to $\kappa a=1.2$ and $\zeta\omega_0=2.1$.

Finally, the behavior of $C_{\rm elec}$ is shown in Fig. 7 as a function of κa for $\zeta\omega_0=2.1$ and $a\omega_0=2.2$. The dependence on the Debye screening parameter in Eq. (15) comes only from the first term, where the negative sign of the coefficient of $(\kappa a)^2$ causes a dip in the plot for $C_{\rm elec}$ around $\kappa a\approx 1.3$, which by chance corresponds to the normal physiological salt concentration. However, as can be seen from Fig. 7, the dependence of the electrostatic twist rigidity on κa is extremely weak as long as $\kappa<\omega_0$, which is a manifestation of the fact that screening is controlled by the periodic charge distribution and the effective screening length is set by the pitch P, which is shorter than κ^{-1} in this regime (see the discussion below).

It is worth saying a few words about the other limit where $\kappa>\omega_0$, corresponding to high salt concentration. In Eq. (9), one can clearly see that in the nth term in the series there is a competition between κ and $n\omega_0$ to control the screening. If the salt concentration is so high that we have $\kappa>n_c\omega_0$, the periodic structure plays no role and screening is entirely controlled by the Debye screening in the bulk. For relatively strong Debye screening when $\kappa a>1$, we can use the simple asymptotic forms of the Bessel functions and find an asymptotic expression for the electrostatic twist rigidity as

$$C_{\rm elec}=\frac{2\ell_B a^2}{b^2}\sum_{n=1}^{n_c}(1+\cos\, n\omega_0\zeta)\frac{n^2[2(na\omega_0)^2-(\kappa a)^2]}{[(\kappa a)^2+(na\omega_0)^2]^{5/2}}. \tag{16}$$

This expression can be used for the region $\kappa>\omega_0$, where it predicts $C_{\rm elec}>0$ for $\kappa<s\omega_0$, and $C_{\rm elec}<0$ for $\kappa>s\omega_0$, for a value of $s\approx n_c$.

B. Correction to spontaneous twist

Similarly, we can calculate the electrostatic contribution to the spontaneous twist of the charged double helix. To that end, we expand the modified Bessel functions I_n and K_n to the fourth order in $(\kappa a)/(na\omega_0)$, and make use of the relevant asymptotic forms of $I_n(x)$ and $K_n(x)$ for $n\geqslant 2$. We find

$$W_{\rm elec}=\frac{4\ell_B a}{b^2}(1+\cos\,\omega_0\zeta)\times[g_0(a\omega_0)-g_2(a\omega_0)(\kappa a)^2+g_4(a\omega_0)(\kappa a)^4]-\frac{4\ell_B a}{b^2}\left[\gamma+\ln\frac{n_c}{2\,\sin(\omega_0\zeta/2)}-(1+\cos\omega_0\zeta)\right], \tag{17}$$

where the summation on n has been performed using the cutoff n_c, as discussed in Sec. III A. Note that the above result is valid only for $\kappa<\omega_0$.

By defining $W_0\equiv 4\ell_B a/b^2$ and using the geometrical parameters for B-DNA (see Sec. III A above), we find $W_0=29.5$. So Eq. (17) yields $W_{\rm elec}=-11.1$ at a physiological salt concentration ($\kappa\approx 1$ nm^{-1}).

Let us now study the behavior of $W_{\rm elec}$ as a function of $a\omega_0$, κa, and $\zeta\omega_0$. In Fig. 8, the dependence of $W_{\rm elec}$ is shown on the parameter $a\omega_0$ for $\kappa a=1.2$ and $\zeta\omega_0=2.1$. The plot shows that for sufficiently high salt concentration the electrostatic correction to the spontaneous twist increases as the mechanical spontaneous twist of the double helix increases.

In Fig. 9, the behavior of $W_{\rm elec}$ is shown as a function of $a\omega_0$ for $\kappa a=1.2$ and $\zeta\omega_0=2.1$. One can see that, contrary to the $C_{\rm elec}$ case, $W_{\rm elec}$ never changes its sign and it is always negative.

In Fig. 10, the dependence of $W_{\rm elec}$ on the asymmetry parameter $\zeta\omega_0$ is sketched, for $\kappa a=1.2$ and $a\omega_0=2.2$. As in the $C_{\rm elec}$ case, for the relatively large window of $0.4\pi\leqslant\zeta\omega_0\leqslant 1.6\pi$, $W_{\rm elec}$ does not appear to change appreciably, and thus it is not sensitive to the relative positioning of the two strands. For $\zeta\omega_0=0$ and $\zeta\omega_0=2\pi$, there is a divergence in $W_{\rm elec}$ due to the fact that the charges on the two strands come into contact with each other.

Finally, the behavior of $W_{\rm elec}$ is shown in Fig. 11 as a function of κa for $\zeta\omega_0=2.1$ and $a\omega_0=2.2$. As one can see, the dependence of $W_{\rm elec}$ on κa is very weak for $\kappa<\omega_0$,

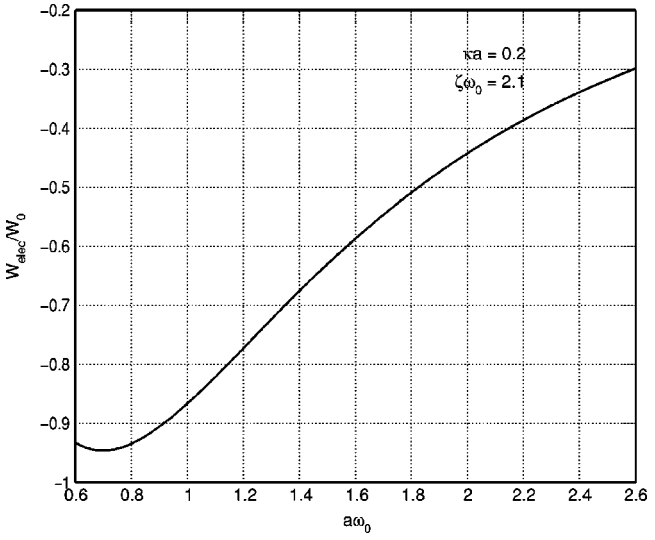

FIG. 9. W_{elec}/W_0 as a function of $a\omega_0$. This plot corresponds to $\kappa a=0.2$ and $\zeta\omega_0=2.1$.

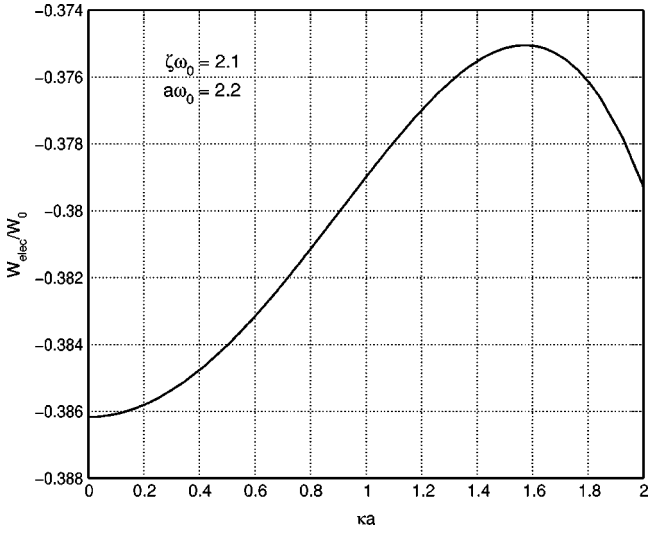

FIG. 11. W_{elec}/W_0 as a function of κa. This plot corresponds to $\zeta\omega_0=2.1$ and $a\omega_0=2.2$.

which is due to the fact that the screening is controlled by the periodic charge distribution in this regime.

In the opposite limit where $\kappa > \omega_0$, corresponding to high salt concentration, one can again use the appropriate limiting form of the Bessel functions, and find W_{elec} as

$$W_{\mathrm{elec}} = -\frac{2\ell_B a}{b^2}\sum_{n=1}^{n_c}(1+\cos n\omega_0\zeta)\frac{n^2 a\omega_0}{[(\kappa a)^2+(na\omega_0)^2]^{5/2}} \tag{18}$$

to the leading order. This expression confirms that W_{elec} is also negative in the highly screened case. The facts that the electrostatic contribution to the spontaneous twist is negative and that DNA tends to undertwist because of electrostatics can be understood as being a result of the electrostatic repulsion between the charges along the backbone.

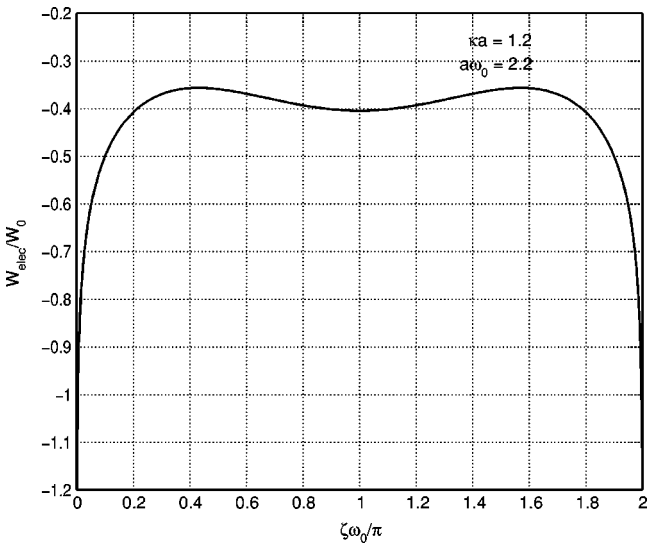

FIG. 10. W_{elec}/W_0 as a function of $\zeta\omega_0$. This plot corresponds to $\kappa a=1.2$ and $a\omega_0=2.2$.

IV. DISCUSSION

For a polyelectrolyte with a periodic spatial charge distribution, such as the double-helical structure of DNA, there are two competing mechanisms for screening the electrostatic self-interaction and its contribution to the twist rigidity: the *Debye screening* due to the free ions in the solution, and the *structural screening* caused by the periodic structure of the charge distribution; a periodic charge distribution leads to an electric potential that decays exponentially. While the screening length for the former case is set by the Debye length κ^{-1}, it is set by the period P of the charge distribution in the latter, and the dominant mechanism corresponds to the one with the shorter screening length.

It appears that the contribution of electrostatic interactions to twist rigidity can be either negative or positive, depending on the parameters. The negative values for the electrostatic torsional stiffness could lead to instability in the structure of the helical polyelectrolyte, depending on whether the mechanical structure of the macromolecule can counterbalance the effect of the electrostatic instability. We have used this criterion in Fig. 2 to summarize these different regimes in the parameter space. Considering that a helical polyelectrolyte seems to be the general structure of many stiff biopolymers (such as DNA and actin filaments) it is interesting to know which helical configurations can in principle lead to stable structures, and which ones cannot. This could be especially important in the case of biopolymers that self-assemble through polymerization processes, such as actin filaments, where such energetic considerations could hamper or favor the polymerization process. Note that the onset of instability can only suggest that the structure will tumble into another configuration, and determining the final stable structure requires knowledge of other interactions.

The twist rigidity of *B*-DNA is believed to be roughly 75 nm [14], which should be thought of as the sum of the

mechanical and the electrostatic contributions: $C=C_{\mathrm{mech}}+C_{\mathrm{elec}}$. Our estimate of $C_{\mathrm{elec}}\approx 5$ nm reveals that about 7% of the twist rigidity of DNA is due to electrostatic interactions. This result is more or less independent of the salt concentration, as the dependence of C_{elec} on salt concentration is very weak. For example, the difference between C_{elec} at zero and very high salt concentration is about 3.5 Å. Therefore $\Delta C_{\mathrm{elec}}/C=0.5\%$, which is very small. While this naturally explains why in experiments no sensitivity to the salt concentration has been observed, it certainly does not mean that the electrostatic contribution to C is negligible.

In expanding the energy expression around the minimum energy configuration, we have used the spontaneous twist of ω_0 as the reference point [see Eqs. (10) and (13)], as opposed to the preferred value due to the combination of the mechanical and the electrostatic contributions. One can show that the renormalized spontaneous twist is given as $\omega=\omega_0-\Delta\omega$ with $\Delta\omega=W_{\mathrm{elec}}/C_{\mathrm{mech}}$ to the leading order. Putting in numbers, we find $\Delta\omega\approx -0.16$ nm^{-1}, which means that the overall correction for the spontaneous twist of *B*-DNA is at least one order of magnitude smaller than ω_0, and thus it will not affect the obtained results to the leading order. So it would be a good approximation to estimate the electrostatic contribution to the twist rigidity at ω_0.

Screening effects are the result of the interaction between polyelectrolyte charges and the mobile charges in the solvent. In a very dilute solution, the screening problem can be treated by considering the electrostatic potential around a polyelectrolyte chain, which can be obtained by solving the Poisson-Boltzmann equation. For high salt concentration, the screening will be very strong and the Debye-Hückel equation, which is a linearized approximation of the Poisson-Boltzmann equation, yields a sufficiently accurate description of the screening potential. In the case of weak screening, however, the Poisson-Boltzmann equation predicts that the counterions accumulate nearby the polyelectrolyte; a phenomenon termed counterion condensation. In this case, it has been shown that an effective description in which a condensed layer of counterions is assumed in the immediate vicinity of the polyelectrolyte (with the major effect of renormalizing the surface charge density) and a coupled Debye-Hückel screening in the bulk is a good approximation to the nonlinear Poisson-Boltzmann screening [15–17].

Let us now try to elaborate on the effect of counterion condensation. For double-stranded DNA, the charge density is sufficiently high such that counterions will condense on the DNA, where they are confined near the sugar-phosphate backbone [18]. The condensed layer of counterions can develop three kinds of ordering depending on the competition between electrostatic correlations, substrate interactions, and thermal fluctuations [19]. If the substrate interaction is so strong that the counterions are bound to be adsorbed onto specific sites and stay there, then the counterion layer couples to the substrate charge distribution and makes a commensurate ordered structure. This will be the case, for example, when the *p*H is changed and the H^+ counterions neutralize some of the phosphate groups of DNA. In this case, the effect of counterion condensation on the electrostatic twist rigidity can be taken into account by simply using the effective distance between neighboring charges b_{eff} instead of b in the present analysis.

When the electrostatic correlations dominate, counterions may form an ordered Wigner liquid in which the layer is completely decorrelated from the underlying substrate. In this case, the presence of the counterion layer does not have an effect on the electrostatic twist rigidity due to lack of coupling. This is also the case when thermal fluctuations wash out all the ordering, again because the counterion layer is decoupled from the substrate charge distribution.

When the pitch of the DNA is changed, the linear charge density will change because the same number of charges will be distributed on a different length. Therefore, the amount of condensed ions on the rod will change, which will make an entropic contribution to the twist rigidity. The electrostatic free energy of a charged rod above the threshold of counterion condensation can be written as [15,20] $\beta F\simeq(N/\xi)\ln(\kappa a)$ where N is the total number of monovalent charges on the rod and ξ is the Manning parameter, that is defined as $\xi=\ell_{\mathrm{B}}/(P/n_0)$, where n_0 is the number of negative charges on one pitch of the double-helical polyelectrolyte ($n_0=20$ for DNA). This leads to a contribution to twist rigidity due to counterion condensation, that is given by $C_{\mathrm{cond}}\approx(2/\ell_{\mathrm{B}}\omega_0^2)\ln(\kappa a)$. For the physiological condition, we have $C_{\mathrm{cond}}\approx 1.5$ Å, which is much smaller than C_{elec}, and thus the entropic effect is negligible.

The effect of dielectric discontinuity in the vicinity of the polyelectrolyte has been neglected in the present analysis. The interior of DNA has a very low dielectric constant and the contrast with the bulk dielectric constant (which is about 80) can affect the electrostatic self-interaction. This effect has been studied in the case of DNA, and it has been shown that it will enhance counterion condensation by effectively strengthening the substrate potential to such an extent that the counterion layer will become commensurate with the double-helical backbone [18]. In this case, one can incorporate the effect of the dielectric discontinuity by using a corresponding b_{eff}, as discussed above. Another effect of a low dielectric constant in the interior would be the appearance of image charges, which would slightly enhance the electrostatic self-energy.

In the above analysis we have assumed that imposing a finite angle of twist between the two ends of a helical polyelectrolyte leads to a uniform twist. This is analogous to the assumption of uniform bending made by Odijk when calculating the electrostatic bending rigidity, and presumably holds true when the effective elasticity due to electrostatics is local. In Ref. [21], this assumption was scrutinized, and it was shown that this assumption is valid provided one of these conditions holds: (1) the polyelectrolyte segment is long, (2) the Debye screening is strong, (3) the charging is weak, or (4) the mechanical stiffness of the polyelectrolyte is larger than the electrostatic contribution. We expect the same argument to hold true for the twist rigidity as well. Since for the case of DNA we have shown that the mechanical twist rigidity is much larger than the electrostatic contribution, we can safely assume that the twist is uniform.

In conclusion, we have studied the electrostatic contribution to the twist rigidity of DNA, taking into account its dependence on the salt concentration in the solvent. We have shown that there is a non-negligible electrostatic contribution to the twist rigidity, which varies very slowly on changing

the salt concentration in the solution. By changing the geometrical parameters of the helix and the Debye screening length, the electrostatic twist rigidity can change sign and become negative, implying that a helical structure could be a stable as well as an unstable configuration for a helical polyelectrolyte. We finally note that the present analysis can be also applied to other biopolymers such as *F*-actin.

ACKNOWLEDGMENT

We are grateful to T. B. Liverpool for interesting discussions and comments.

APPENDIX A: COULOMB ENERGY IN FOURIER SPACE

Due to the periodicity of the charge distribution, it is convenient to calculate the electrostatic self-energy in Eq. (1) in Fourier space. We start from the Fourier representation of the screened Debye-Hückel interaction in Eq. (2):

$$\beta E_{\rm elec} = \frac{a^2}{2}\int \frac{d^3k}{(2\pi)^3}\int dz dz' \int_0^{2\pi} d\theta d\theta' \sigma(z,\theta)\sigma(z',\theta') \times \frac{4\pi\ell_{\rm B}}{k^2+\kappa^2} e^{i\vec{k}\cdot[\vec{r}(z,\theta)-\vec{r}(z',\theta')]}. \tag{A1}$$

Using cylindrical coordinates, we can write $\vec{r}(z,\theta)=z\hat{z}+a(\cos\theta\hat{x}+\sin\theta\hat{y})$, which in conjunction with $\vec{k}=k_z\hat{z}+k_\perp(\cos\phi\hat{x}+\sin\phi\hat{y})$, yields

$$\begin{aligned}\beta E_{\rm elec} = {} & \frac{\ell_{\rm B}a^2}{2}\int dz dz' \int_0^{2\pi} d\theta d\theta' \\ & \times \int_{-\infty}^{+\infty}\frac{dk_z}{2\pi}\int_0^{\infty}\frac{k_\perp dk_\perp}{(2\pi)^2}\int_0^{2\pi} d\phi \sum_{m,n}\sum_{m',n'}\sigma_{m,n}\sigma_{m',n'} \\ & \times \frac{4\pi}{k_z^2+k_\perp^2+\kappa^2} e^{i(2\pi m/P+k_z)z+in\theta+ik_\perp a\,\cos(\phi-\theta)} \\ & \times e^{i(2\pi m'/p-k_z)z'+in'\theta'-ik_\perp a\,\cos(\phi-\theta')}.\end{aligned} \tag{A2}$$

After integration over z, z', and k_z, we find

$$\begin{aligned}\beta E_{\rm elec} = {} & \frac{\ell_{\rm B}a^2}{2}\int_0^{2\pi} d\theta d\theta' d\phi \int_0^{\infty}\frac{k_\perp dk_\perp}{(2\pi)^2} \\ & \times \sum_{m,n}\sum_{m',n'}\sigma_{m,n}\sigma_{m',n'}\frac{4\pi L\,\delta_{m,-m'}}{(2\pi m/P)^2+k_\perp^2+\kappa^2} \\ & \times e^{i(n\theta+n'\theta')+iak_\perp[\cos(\phi-\theta)-\cos(\phi-\theta')]}.\end{aligned} \tag{A3}$$

By defining $\theta=\theta_1+\phi$ and $\theta'=\theta_2+\phi$, the integration over the three angles in Eq. (A3) can be performed as

$$\begin{aligned}\int d\theta d\theta' d\phi e^{i(n\theta+n'\theta')+iak_\perp[\cos(\phi-\theta)-\cos(\phi-\theta')]} \\ = (2\pi)^3\delta_{n,-n'}[J_n(k_\perp a)]^2,\end{aligned} \tag{A4}$$

to yield

$$\beta E_{\rm elec} = 4\pi^2\ell_{\rm B}La^2\sum_{m,n}|\sigma_{m,n}|^2\int_0^{\infty} dk_\perp k_\perp \frac{J_n^2(k_\perp a)}{(2\pi m/P)^2+k_\perp^2+\kappa^2}. \tag{A5}$$

Performing the final integration over $k_\perp$ using [22]

$$\int_0^{\infty}\frac{x}{x^2+h^2}[J_\nu(x)]^2dx = I_\nu(h)K_\nu(h), \tag{A6}$$

we obtain the result quoted in Eq. (5).

APPENDIX B: ASYMPTOTIC FORMS OF THE BESSEL FUNCTIONS

In this appendix, the asymptotic forms of $I_n(nx)$ and $K_n(nx)$ for large n are derived. We use the integral representation of these functions:

$$\begin{aligned}I_n(nx) &= \frac{1}{\pi^{1/2}(n-1/2)!}\left(\frac{nx}{2}\right)^n\int_{-1}^{+1} dp e^{nxp}(1-p^2)^{n-1/2}, \\ K_n(nx) &= \frac{\pi^{1/2}}{(n-1/2)!}\left(\frac{nx}{2}\right)^n\int_{1}^{\infty} dp e^{-nxp}(p^2-1)^{n-1/2}.\end{aligned} \tag{B1}$$

Let us first consider the case of $I_n(nx)$. We denote

$$Q \equiv \int_{-1}^{+1} dp\; e^{nxp}(1-p^2)^{n-1/2} = \int_{-1}^{+1} dp e^{g(p)} \tag{B2}$$

and expand $g(p)$ around p_0, the position of its maximum, to second order of $(p-p_0)$, as

$$\begin{aligned}g(p) &\simeq g(p_0)+\frac{1}{2}f''(p_0)(p-p_0)^2 \\ &= nxp_0+\left(n-\frac{1}{2}\right)\ln(1-p_0^2)-\left(n-\frac{1}{2}\right)\frac{1+p_0^2}{(1-p_0^2)^2}(p-p_0)^2,\end{aligned} \tag{B3}$$

where

$$p_0 = \frac{-1+\sqrt{1+x^2}}{x}+\frac{1}{2nx}\left(1+\frac{1}{\sqrt{1+x^2}}\right). \tag{B4}$$

Using this form for $g(p)$, Q can be found as

$$Q \simeq \frac{1-p_0^2}{\sqrt{n(1+p_0^2)}}e^{nxp_0+(n-1/2)\ln(1-p_0^2)}. \tag{B5}$$

Finally, using Stirling's formula for $n!$, we find

$$\begin{aligned}I_n(nx) \simeq {} & \frac{1}{\sqrt{2\pi}}\frac{1-p_0^2}{\sqrt{n(1+p_0^2)}} \\ & \times e^{(n-1/2)\ln(1-p_0^2)+nxp_0+n[1+\ln(x/2)]+1/24n}.\end{aligned} \tag{B6}$$

Using a similar treatment, we find the large n asymptotic behavior for $K_n(nx)$ as

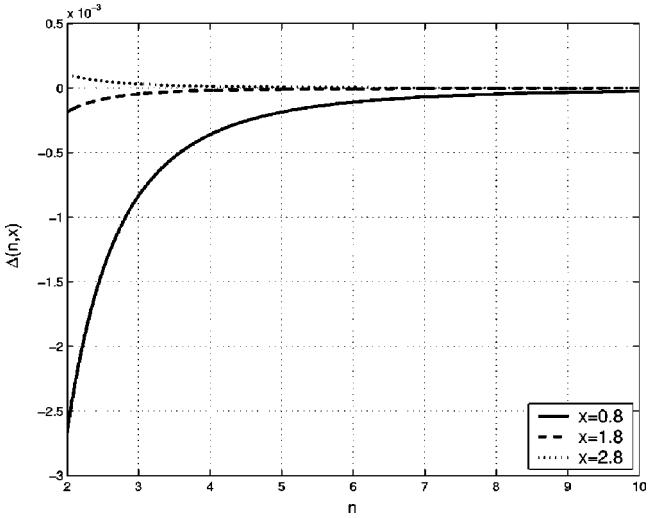

FIG. 12. Difference between the asymptotic form of $I_n(nx)K_n(nx)$ and its exact value as a function of n for several values of x. The solid line corresponds to $x=0.8$, the dashed line corresponds to $x=1.8$, and the dotted line corresponds to $x=2.8$. The difference is less than 0.25%.

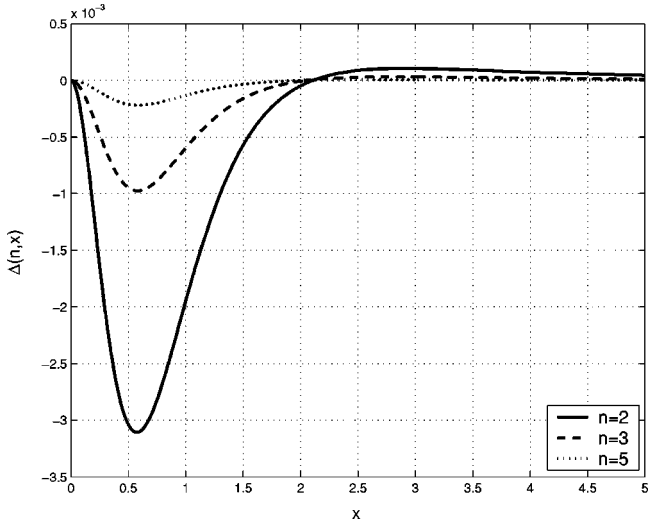

FIG. 13. Difference between the asymptotic form of $I_n(nx)K_n(nx)$ and its exact value as a function of x for different values of n. The solid line corresponds to $n=2$, the dashed line corresponds to $n=3$, and the dotted line corresponds to $n=5$. The difference is less than 0.3%.

$$K_n(nx) \simeq \frac{1}{\sqrt{2n}} \frac{p_0'^2 - 1}{\sqrt{n(1+p_0'^2)}} \times e^{t(n-1/2)\ln(p_0'^2-1) - nxp_0' + n[1+\ln(x/2)]+1/24n}, \quad \text{(B7)}$$

where

$$p_0' = \frac{1+\sqrt{1+x^2}}{x} - \frac{1}{2nx}\left(1 + \frac{1}{\sqrt{1+x^2}}\right). \quad \text{(B8)}$$

By using these relations for $I_n(nx)$ and $K_n(nx)$, we find

$$I_n(nx)K_n(nx) = \frac{1}{2\sqrt{1+x^2}}\frac{1}{n} + O\left(\frac{1}{n^{2+\delta}}\right), \quad \text{(B9)}$$

where $\delta \geqslant 0$.

We define $\Delta(n,x) \equiv I_n(nx)K_n(nx) - 1/2n\sqrt{1+x^2}$ and in Fig. 12 show the behavior of $\Delta(n,x)$ as a function of n for several values of x. As can be seen, the difference is less than 0.25% in the worst case, which implies that the asymptotic form of $I_n(nx)K_n(nx)$ for $n \geqslant 2$ can be used as a good approximation for the range of x we are interested in.

In Fig. 13, we show the behavior of $\Delta(n,x)$ as a function of x for different values of n. This plot shows that for $n \geqslant 2$ the difference goes to zero as x increases.

APPENDIX C: THE EXPLICIT FORMS OF THE AUXILIARY FUNCTIONS

In this appendix, we give the explicit forms of the auxiliary functions used in Eqs. (14), (15), and (17), above. The function $f_0(x)$ reads

$$f_0(x) = 4\left(1 + \frac{1}{x^2}\right) I_1(x)K_1(x) + 4I_1'(x)K_1'(x) - \frac{2}{x}[I_1(x)K_1'(x) + I_1'(x)K_1(x)], \quad \text{(C1)}$$

where the prime indicates differentiation. One can show that for $x \ll 1$ it behaves as $f_0(x) = \ln x + O(x^2 \ln x)$. The second function $f_2(x)$ is written as

$$f_2(x) = -3\left(\frac{1}{x} + \frac{1}{x^3}\right)[I_1(x)K_1'(x) + I_1'(x)K_1(x)] + \frac{1}{x}[I_1'(x)K_2'(x) - I_2'(x)K_1'(x)] + \frac{3}{x^2}[I_1(x)K_1(x) - 2I_1'(x)K_1'(x)] + \frac{3}{2x^2}[I_2'(x)K_1(x) - I_1(x)K_2'(x)] + \frac{2}{x^3}[I_1(x)K_2(x) - I_2(x)K_1(x)], \quad \text{(C2)}$$

and for $x \ll 1$ it behaves as $f_2(x) = 1/(2x^2) - \ln x/2 + O(x^2 \ln x)$. Finally, for $f_4(x)$ we have

$$f_4(x) = \frac{176 + 136x^2 + 19x^4}{16x^6} I_1(x)K_1(x) - \frac{7}{8x^3}[I_3(x)K_1'(x) + I_1'(x)K_3(x)] + \frac{1}{x^4}[I_2(x)K_1'(x) - I_1'(x)K_2(x)] + \frac{11+2x^2}{x^4} I_1'(x)K_1'(x) + \frac{1}{16x^2} I_3(x)K_3(x) + \frac{14+3x^2}{8x^4}[I_2'(x)K_1(x) - I_1(x)K_2'(x)] - \frac{88+49x^2}{8x^5}[I_1'(x)K_1(x) + I_1(x)K_1'(x)]$$

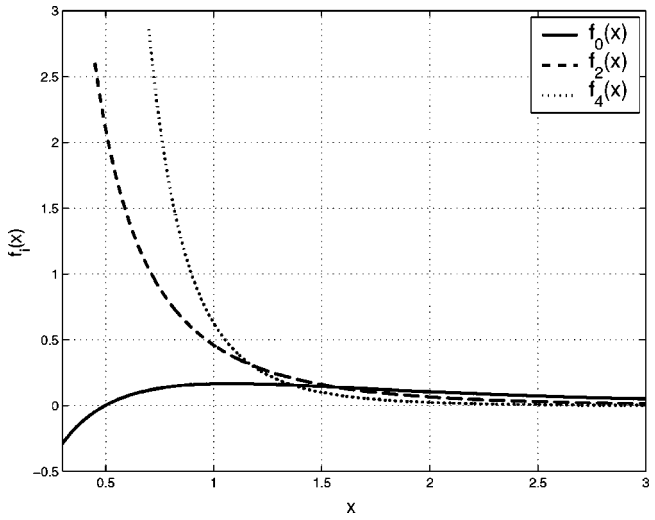

FIG. 14. The auxiliary functions $f_0(x)$, $f_2(x)$, and $f_4(x)$.

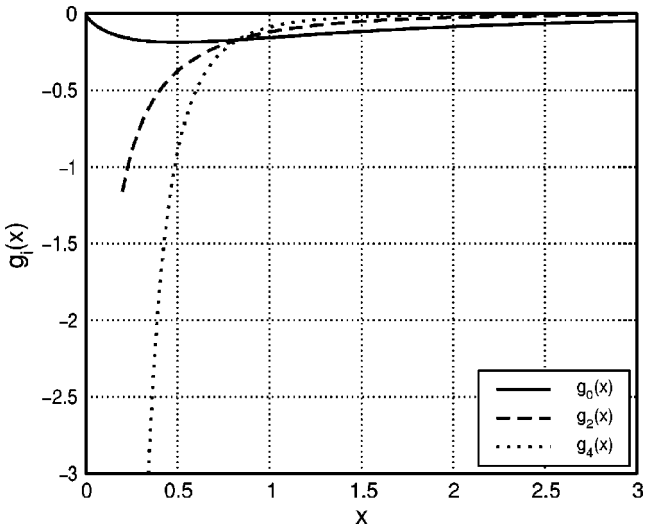

FIG. 15. The auxiliary functions $g_0(x)$, $g_2(x)$, and $g_4(x)$.

$$-\frac{1}{x^5}[I_2(x)K_1(x)-I_1(x)K_2(x)], \tag{C3}$$

which behaves as $f_4(x)=3/(4x^4)-1/(8x^2)+5/64\ \ln x+O(x^2\ \ln x)$, for $x\ll 1$. At infinity, all of these functions go to zero faster than $1/x^2$, with $f_4(x)$ vanishing faster than $f_2(x)$, and $f_2(x)$ faster than $f_0(x)$. (See Fig. 14).

The function $g_0(x)$ is given by

$$g_0(x)=I_1'(x)K_1(x)+I_1(x)K_1'(x), \tag{C4}$$

where the prime indicates differentiation. It is simple to show that for $x\ll 1$ it behaves as $g_0(x)=\frac{1}{8}(1+4\gamma-4\ \ln 2)x+\frac{1}{2}x\ \ln x+O(x^3)$ and for $x\gg 1$ it behaves as $g_0(x)=-1/2x^2+O(1/x^4)$. The function $g_2(x)$ is written as

$$g_2(x)=\frac{1}{2x^2}[I_1(x)K_1'(x)+I_1'(x)K_1(x)]-\frac{1}{2x}[I_1(x)K_1(x)+I_1'(x)K_1'(x)]-\frac{1}{4x}[I_2'(x)K_1(x)-I_1(x)K_2'(x)], \tag{C5}$$

which behaves as $g_2(x)=-1/(4x)+O(x)$ for $x\ll 1$ and as $g_2(x)=-3/(4x^4)+O(1/x^6)$ for $x\gg 1$. Finally, for $g_4(x)$ we have

$$g_4(x)=\frac{1}{x^2}[I_1'(x)K_1(x)+I_1(x)K_1'(x)]+\frac{1}{3x^2}[I_2'(x)K_1'(x)-I_1'(x)K_2'(x)]-\frac{1}{4x^3}[4I_1'(x)K_1'(x)+3I_1(x)K_1(x)]-\frac{1}{8x^3}[I_2'(x)K_1(x)-I_1(x)K_2'(x)]+\frac{1}{x^4}[I_1'(x)K_1(x)+I_1(x)K_1'(x)]-\frac{1}{x^5}I_1(x)K_1(x), \tag{C6}$$

which behaves as $g_4(x)=-1/(8x^3)+1/(16x)+O(x)$ for $x\ll 1$, and as $g_4(x)=-15/(16x^6)+O(1/x^8)$ for $x\gg 1$. In Fig. 15, we show the behavior of $g_i(x)$ as a function of x.

[1] B. Alberts, A. Johnson, J. Lewis, M. Raff, K. Roberts, and P. Walter, *Molecular Biology of the Cell* (Garland, New York, 2002).

[2] V. A. Bloomfield, D. M. Crothers, and I. Tinoco, Jr., *Nucleic Acids: Structure, Properties, and Functions* (University Science Books, Sausalito, CA, 2000).

[3] T. Odijk, J. Polym. Sci. [A1] **15**, 477 (1977).

[4] J. Skolnick and M. Fixman, Macromolecules **10**, 944 (1977).

[5] For a review on polyelectrolyte elasticity, see J.-L. Barrat and J.-F. Joanny, *Polymeric Systems, Advances in Chemical Physics*, Vol. 94, edited by I. Prigogine and S. A. Rice (John Wiley, New York, 1996).

[6] M. D. Wang, H. Yin, R. Landick, J. Gelles, and S. M. Block, Biophys. J. **72**, 1335 (1997).

[7] C. G. Baumann, S. B. Smith, V. A. Bloomfield, and C. Bustamante, Proc. Natl. Acad. Sci. U.S.A. **94**, 6185 (1997).

[8] P. J. Hagerman, Biopolymers **22**, 811 (1983).

[9] W. H. Taylor and P. J. Hagerman, J. Mol. Biol. **212**, 363 (1990).

[10] R. D. Kamien, T. C. Lubensky, P. Nelson, and C. S. O'Hern, Europhys. Lett. **38**, 237 (1997).

[11] E. J. W. Verwey and J. Th. G. Overbeek, *Theory of the Stability of Lyophobic Colloids* (Elsevier, New York, 1948).

[12] L. Landau and E. Lifshitz, *Theory of Elasticity*, 3rd ed. (Per-

gamon, Oxford, 1986).
[13] R. P. Feynman, R. Leighton, and M. Sands, *The Feynman Lectures on Physics*, Vol. 2 (Addison-Wesley, Reading, MA, 1975).
[14] A. V. Vologodskii, S. D. Levene, K. V. Klenin, M. Frank-Kamenetskii, and N. R. Cozzarelli, J. Mol. Biol. **227**, 1224 (1992); J. F. Marko and E. D. Siggia, Phys. Rev. E **52**, 2912 (1995).
[15] F. Oosawa, *Polyelectrolytes* (Marcel Dekker, New York, 1971).
[16] G. S. Manning, J. Chem. Phys. **51**, 954 (1969).
[17] S. Alexander, P. M. Chaikin, P. Grant, G. J. Morales, P. Pincus, and D. Hone, J. Chem. Phys. **80**, 5776 (1984).
[18] V. Bloomflied and I. L. Carpenter, in *Polyelectrolytes Science and Technology*, edited by M. Hara (Marcel Dekker, New York, 1993).
[19] R. Golestanian and T. B. Liverpool, Phys. Rev. E **66**, 051802 (2002).
[20] A. Naji, R. R. Netz, and C. Seidel, Eur. Phys. J. E **12**, 223 (2003).
[21] R. Zandi, J. Rudnick, and R. Golestanian, Eur. Phys. J. E **9**, 41 (2002); R. Zandi, J. Rudnick, and R. Golestanian, Phys. Rev. E **67**, 021803 (2003); R. Zandi, J. Rudnick, and R. Golestanian, Phys. Rev. E **67**, 061805 (2003).
[22] I. S. Gradshteyn and I. M. Ryzhik, *Table of Integrals, Series, and Products*, 6th ed. (Academic Press, New York, 2000).